

# Radio-frequency magnetic response of vortex lattices undergoing structural transformations

R. Prozorov,\* V. G. Kogan, M. D. Vannette, S. L. Bud'ko, and P. C. Canfield

*Ames Laboratory and Department of Physics and Astronomy, Iowa State University, Ames IA 50011, USA*

(Dated: 21 February 2007)

We report a clear anomaly in the rf response of a tunnel-diode resonator measured in borocarbide crystals in dc fields along the  $c$ -axis. We associate the anomaly in the dynamic magnetic susceptibility,  $\chi$ , with a structural transition in the vortex lattice.  $\chi$  is sensitive to the Campbell penetration depth  $\lambda_C$  of the rf perturbation into the mixed state.  $\lambda_C$  depends on the vortex lattice elastic moduli, which in turn depend on the vortex lattice structure. The high-field transition line is clearly mapped and shown to behave in agreement with theory.

PACS numbers: PACS: 74.25.Nf, 74.25.Qt, 74.25.Sv, 74.70.Dd

In the classical picture of type-II superconductors, vortices should form a hexagonal lattice in isotropic or cubic materials; the same should happen in tetragonal materials for applied magnetic fields along the crystallographic  $c$  axis. It has been known for a long time that experimentally this is rarely the case [1, 2]. The reason for such behavior was, to a large extent, clarified after the nonlocal effects were incorporated into the London description of intervortex interaction [3, 4, 5]. This effort resulted in the realization that the vortex lattice (VL) structure depends on the Fermi surface, the order parameter symmetry, as well as on the applied field, temperature, scattering strength, and even on thermal fluctuations of vortex positions [6]. Currently, vortex lattices structural phase transitions are best studied in the rare earth-nickel-borocarbides [7, 8, 9, 10, 11, 12, 13, 14, 15], but in fact present in many superconductors including cubic Nb or  $V_3Si$  [16, 17, 18].

Hence, in addition to boundaries of different dynamic behavior (e.g., liquid, glass, or the “Abrikosov crystal”), the phase diagram of the vortex state contains lines separating different periodic structures within the domain of the Abrikosov crystal. Information about these structures is consequential because the VL elastic properties are structure dependent, whereas the dynamic behavior is affected by the lattice elastic moduli [19].

Vortex lattices have been probed by Bitter decoration [13], Small Angle Neutron Scattering (SANS) [7, 8, 9, 10, 12], and by Scanning Tunneling Microscopy [11, 14]. (Hereafter we are talking about tetragonal crystals in fields along the  $c$ -axis). Notwithstanding considerable progress made in locating the transition lines in low fields (an example is given in Fig. 3), the complete mapping of transitions had proven elusive mostly due to poor high-field sensitivity of these techniques. Calculations based on the Ginzburg-Landau approach [11] suggested that the transition line for transformation of rhombic (triangular) to square (R-S) structures may end up at the upper critical field  $H_{c2}(T)$ . However the SANS data on  $LuNi_2B_2C$  have shown the transition line bending away of  $H_{c2}(T)$  [15]. Gurevich and Kogan [6] suggested that

softening of the lattice near  $H_{c2}(T)$  causes the vortex fluctuations to increase thus smearing a weak square-symmetric intervortex interaction and making it isotropic (see also [20]). The model predicts that in small fields the R-S transition line  $H_{\square}(T)$  slowly increases with temperature but then sharply turns upward to avoid  $H_{c2}(T)$  and become a double-valued function.

The dynamic magnetic susceptibility  $\chi$  of a superconductor in the mixed state can be measured by the tunnel-diode resonator technique described elsewhere [21, 22]. In short, the frequency shift,  $\Delta f$ , due to a small change in the resonator induction caused by the finite penetration of the ac field into the sample in the mixed state is recorded. This shift is proportional to the change in the total rf penetration depth,  $\delta \propto \Delta f$  as long as  $\delta$  is smaller than the sample size. In the limit of small amplitude ac excitation fields (0.02 Oe in our case), the non-dissipative part  $\text{Re } \chi$  is determined by the ac field penetration depth  $\delta = (\lambda^2 + \lambda_C^2)^{1/2}$ , where  $\lambda$  is the London penetration depth and the Campbell length  $\lambda_C$  characterizes the pinning and the VL elastic response [23, 24]. For  $f \sim 10$  MHz, the skin-depth due to the normal excitations vastly exceeds the size of our samples and has no effect on  $\delta$ . In this work we utilize the sensitivity of this method to small changes in  $\lambda_C$  that accompany the VL transitions to map the high-field part of the  $H_{\square}(T)$  line unattainable by other techniques.

$LuNi_2B_2C$  (Lu1221) were grown out of  $Ni_2B$  flux [12, 25]. Powder X-ray diffraction spectra indicate that there were no detectable second phases present.  $YNi_2B_2C$  was grown using vertical zone melting method with a commercial 4-mirrors image furnace (model FZ-T-4000-H-VI-VPM-PC, Crystal Systems Corp., Japan). We have studied both as grown and annealed in active vacuum (950°C, 48 h) samples [26] of a typical size  $1 \times 1 \times 0.1$  mm<sup>3</sup>. Residual resistance ratios (RRR) of Lu-1221 and Y-1221 were about 25, the critical temperatures  $T_c \approx 16.2$  and 15.2 K and the upper critical fields  $H_{c2} \approx 9.2$  and 8.8 T, respectively.  $H_{c2}$  was determined as the onset point of the diamagnetic signal. Similar values were obtained from resistivity onset as well as ex-

trapolation technique used in Ref.[25].

The temperature scans of the dynamic susceptibility  $\text{Re}\chi$  at fixed dc fields from 0 to 8 T for the Y-1221 single crystal with  $H_{dc}||H_{ac}$  along the  $c$  axis are shown in Fig. 1. Hereafter we deal only with  $\text{Re}\chi$  and omit “Re” for brevity; - this quantity is normalized so as to have  $-1/4\pi$  in the limit  $H_{dc} \rightarrow 0$  and to correspond to the full expulsion of the ac signal for  $\delta$  small relative to the sample size. There are clear anomalies in high-field scans the locus of which appear as a continuous line. The inset to Fig.1 shows magnetic field scans at constant  $T$  with a clearly visible anomaly. The positions  $(H, T)$  of the anomaly in field sweeps coincide with those observed in  $\chi(T)$  scans. The field  $H_{c2}(T)$  can also be extracted from the data as points where  $\chi$  first deviates from the upper envelop corresponding to the normal state skin effect; the observed anomaly clearly differs from  $H_{c2}$ .

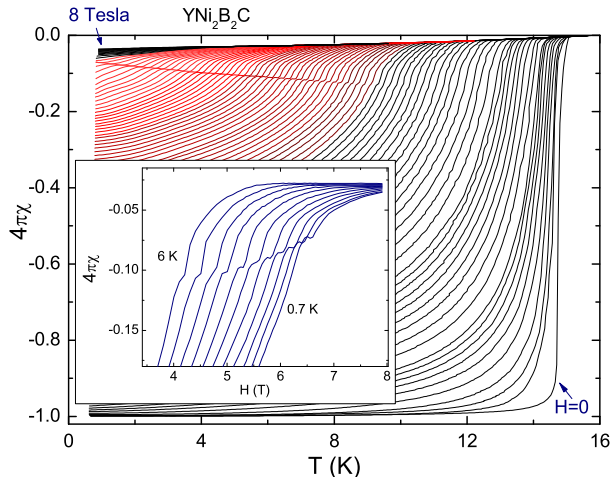


FIG. 1: (Color online)  $\chi(T)$  in Y1221 measured in fixed fields with 1 kOe step. The anomaly corresponding to the VL transition is clearly seen in the upper left corner (region of red color online). *Inset*:  $\chi(H)$  scans showing the same anomaly.

Figure 2 shows  $\chi(T)$  for Y-1221 (upper panel) and Lu-1221 (lower panel) with a focus on low temperatures and high fields where the anomaly clearly seen in both samples. Hence, the observed behavior is not limited to a particular sample, but is seen on both mirror furnace grown Y-1221 and flux-grown Lu-1221.

Figure 3 is a summary of the data in reduced coordinates  $T/T_c$  and  $H/H_{c2}(0)$ . The curves  $H_{c2}/H_{c2}(0)$  are nearly the same for two samples, although as shown in the inset, the absolute values are somewhat different. For comparison, we also show magnetization data of Ref. [27] and the low-field branch of the R-S transition according to SANS measurements of Ref.[15] (shown with the uncertainty corresponding to various criteria for the peaks splitting that mark the R-S transition). The anomaly amplitude decreases with decreasing field and

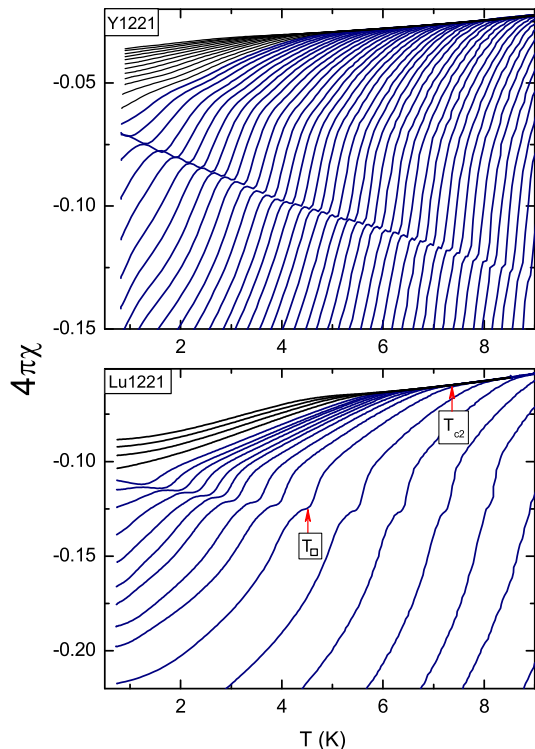


FIG. 2: (Color online) Selected areas of  $\chi(T, H)$  curves showing VL transition in Y1221 (top panel) and Lu1221 (bottom panel). At each field the characteristic temperatures corresponding to  $H_{c2}(T)$  line as well as  $H_{\square}(T)$  are indicated by arrows at the lower frame.

raising temperature (Fig. 2), and the data cannot be extended to the point where they are anticipated to merge with the low field and high temperature SANS results.

The VL response to a small amplitude ac perturbation is determined by the length [23, 24] given by

$$\delta^2 = \lambda^2 + \frac{H^2}{4\pi K} = \lambda^2 + \frac{cH r_p}{4\pi j_c}, \quad (1)$$

where the term containing the Labusch pinning parameter  $K$  is the Campbell’s  $\lambda_C^2$  (in high fields, we do not distinguish between  $H$  and the magnetic induction). In the second formula  $\lambda_C$  is expressed in terms of the disorder length  $r_p$  and the critical current  $j_c$  for the model of *weak collective pinning* expected to hold for high quality crystals of this work [23]. For weak disorder and small  $j_c$ ,  $\lambda \ll \lambda_C$ ; also, one can use the relation  $r_p^2 = \xi^2 + \langle u^2 \rangle$ , where coherence length  $\xi$  is taken to be the range of the pinning potential and  $\langle u^2 \rangle$  is the mean square thermal fluctuation of vortex positions [19].

The VL shear moduli vanish in the limit  $H \rightarrow H_{c2}$ , the lattice softens, and  $\langle u^2 \rangle$  diverges. As argued in [6], the nonlocal corrections to the isotropic intervortex interaction responsible for the square structure are washed away, and the lattice near  $H_{c2}$  is always triangular (for tetrago-

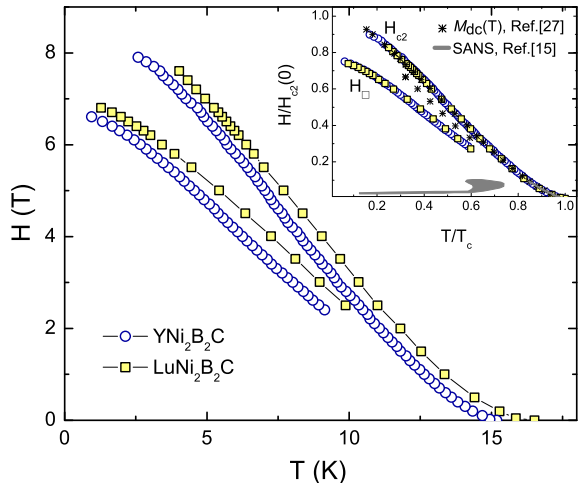


FIG. 3: (Color online) Phase diagram obtained from measurements of  $H_{c2}(T)$  and  $H_{\square}(T)$ . Inset shows the same data in reduced units. Also shown are the results from Refs. [27] and [15].

nal crystals in fields along  $c$  axis). With decreasing field, the fluctuations weaken, and at some field  $H_{\square} < H_{c2}$ , the lattice acquires the square structure. The SANS data on cubic  $V_3Si$  support this picture [18]. It has been estimated in Ref. 6 that this happens when  $\langle u^2 \rangle$  reduces to values on the order  $\xi^2$  for clean materials. In most of the domain  $H_{\square} < H < H_{c2}$ , the fluctuations amplitude exceeds  $\xi$ , and for a qualitative discussion we can take  $r_p^2 \sim \langle u^2 \rangle$ :

$$\delta^2 \approx \frac{cH}{4\pi j_c} \sqrt{\langle u^2 \rangle}. \quad (2)$$

The thermal average  $\langle u^2 \rangle$  depends on *all* VL elastic moduli. The number of independent moduli and their values depend on the lattice structure. For fields small on the  $H_{c2}$  scale, the moduli were counted and evaluated in [28] (and in [20] within the Ginzburg-Landau scheme near  $T_c$ ). The point relevant for our discussion is that the number of independent moduli depends on the symmetry of the lattice (as within the standard elasticity theory for anisotropic solids [29]). When the VL rhombic unit cell with diagonals along [100] and [010] of tetragonal borocarbides (see [4, 9, 10, 11, 14, 15]) transforms to a square, it acquires an extra symmetry associated with the four-fold rotational axis. This reduces the number of independent shear moduli because the shears polarized along [100] and [010] (which are different in the rhombic lattice) become identical. In addition, the squash modulus for the deformation responsible for the transition turns zero at the transition point [20, 28]. One, therefore, expects  $\langle u^2 \rangle$  be different on two sides of the transition point.

The calculation of this difference at the transition in high fields would have required evaluation of the elastic moduli in the presence of thermal fluctuations, a non-trivial problem to be addressed elsewhere. Still, we can state that, with increasing scattering, the domain of the square lattice should shrink and the R-S phase boundary should move to lower reduced fields  $H_{\square}/H_{c2}$  [6]. Physically, this is because the transition to the square structure is caused by the tetragonal symmetry of the Fermi surface and of the order parameter which enter the intervortex interaction through nonlocal corrections to the London theory [3]. In low fields, the corrections add the square symmetric interaction at distances on the order of the nonlocality range  $\rho$  which for clean superconductors is on the order of  $\xi_0$ , zero temperature coherence length. This range, however, shrinks when the mean-free path becomes shorter. Hence, one has to go to higher fields for the square-symmetric interaction to cause the R-S transformation. In the high field domain with fluctuations induced lattice disorder, one has to go to *lower* fields with weaker fluctuations to reach the domain with sufficiently strong nonlocal effects to cause the R-S transition. This happens when  $\rho \sim \langle u^2 \rangle$ . Since  $\rho$  is reduced by scattering, the transition takes place at smaller  $\langle u^2 \rangle$ , i.e., at lower fields.

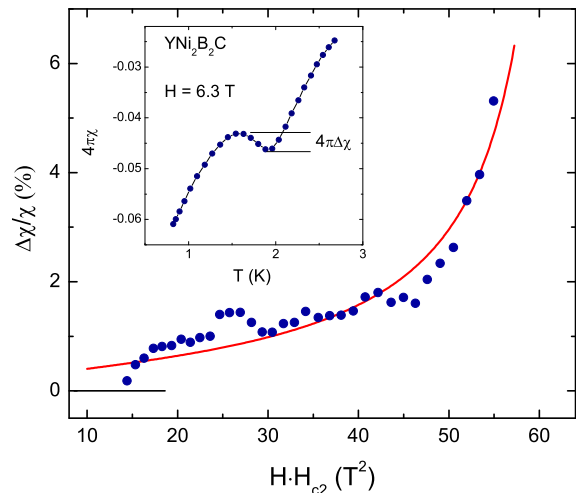


FIG. 4: (Color online) Relative jump in  $\chi$  at the anomaly in  $YNi_2B_2C$  as a function of  $HH_{c2}(T)$ . Solid line is a fit to Eq.(9). *Inset*: the definition of the anomaly size,  $4\pi\Delta\chi$ .

To estimate the dynamic susceptibility we note that in our data  $-4\pi\chi \sim 0.1$  at the location of the transition. This implies that in our case  $\delta$  is comparable or larger than the sample size. A weak screening of the ac field in a disc-shaped sample of a radius  $R$  is described by the London-like equation (see, e.g., [24])  $\mathbf{A} - \delta^2 \nabla^2 \mathbf{A} = 0$  for the vector potential  $\mathbf{A} = \mathbf{h} \times \mathbf{r}/2 + \mathbf{a}$ , where  $\mathbf{a}$  is a small correction to the uniform field. This gives

$$\mathbf{h} \times \mathbf{r}/2 \approx \lambda^2 \nabla^2 \mathbf{a} = -4\pi\delta^2 \mathbf{j}/\mathbf{c}. \quad (3)$$

Given the current  $\mathbf{j}$ , one readily obtains the magnetic moment and  $\chi = -R^2/32\pi\delta^2$ . Hence,

$$-4\pi\chi = \frac{R^2}{8\delta^2} = \frac{\pi R^2 j_c}{2cH} \langle u^2 \rangle^{-1/2}. \quad (4)$$

If  $\langle u^2 \rangle$  varies by  $\Delta\langle u^2 \rangle$ , the change in the measured quantity is:

$$\Delta(-4\pi\chi) = -\frac{\pi R^2 j_c}{4cH \langle u^2 \rangle^{1/2}} \frac{\Delta\langle u^2 \rangle}{\langle u^2 \rangle}. \quad (5)$$

Since  $j_c/\langle u^2 \rangle^{1/2}$  decreases on warming, one expects the anomaly size to decrease with raising  $T$  seen in our data. The relative change in the susceptibility is:

$$\frac{\Delta\chi}{\chi} = -\frac{\Delta\langle u^2 \rangle}{2\langle u^2 \rangle}. \quad (6)$$

At the transition  $\langle u^2 \rangle \sim \xi_0$  for clean materials. As is seen at Fig.4,  $\Delta\chi/\chi \sim 10^{-2}$  in large fields. Hence, our method is sensitive to small changes in thermal averages:  $\sqrt{\Delta\langle u^2 \rangle} \sim \xi_0/10$ .

The elastic properties of the incompressible square lattice in fixed fields are characterized by four independent moduli which can be chosen as the shear  $c_x$  along one of the square diagonals  $x \equiv [100]$ , the squash  $c_s$  transforming the square to a rhombus, the rotation  $c_r$ , and the tilt  $c_{44}$ . At the transition  $c_s = 0$ , whereas according to [6],

$$\frac{c_r}{c_x} \approx \frac{32\pi\rho^2\sqrt{HHc_2}}{\phi_0} \sim \frac{\sqrt{HHc_2(T)}}{Hc_2(0)}, \quad (7)$$

( $\rho$  varies from  $0.67\xi_0$  to  $0.3\xi_0$  on warming from 0 to  $T_c$  in the clean limit). In this situation, Ref. [6] gives  $\langle u^2 \rangle \approx f(H, T) \ln(c_x/c_r)$ , where  $f$  does not depend on elastic moduli. As is shown in [6, 20], only the shear moduli  $c_{66}$  change sharply at the transition, so that we estimate:

$$\frac{\Delta\langle u^2 \rangle}{\langle u^2 \rangle} \sim \frac{\Delta c_{66}}{c_{66} \ln(c_{66}/c_r)} \quad (8)$$

The ratio  $\Delta c_{66}/c_{66}$  should not depend strongly either on  $H$  or on  $T$  since the change of the shear moduli is of a geometric nature (due to the symmetry change). We thus expect the following behavior of the measured quantity:

$$-\frac{\Delta\chi}{\chi} \approx \frac{C}{\ln[Hc_2^2(0)/HHc_2(T)]} \quad (9)$$

with  $C \approx \text{const}$ . Fig.4 shows the data  $\Delta\chi/\chi$  plotted against  $HHc_2(T)$ ; the solid line is calculated taking  $Hc_2(0) = 8.1\text{ T}$  with the fit parameter  $C = 0.75$ . A qualitative nature of our argument notwithstanding, we consider this result as supporting our interpretation of the  $\chi$  anomaly as caused by the R-S structural transformation of the vortex lattice. It should be noted, that the qualitative model we use disregards pinning relative to the thermal fluctuations: the disorder length

$r_p = \sqrt{\xi^2 + \langle u^2 \rangle} \approx \langle u^2 \rangle$ . In the sample with 9% Co, this is unlikely to be true. This might be the reason why the anomaly  $\Delta\chi/\chi$  is nearly washed away in this sample. Large scale inhomogeneities may have the same effect.

A similar claim has been made in Ref. [27] in which an unusual behavior of the reversible magnetization  $M_{dc}(T)$  was interpreted as caused by the R-S transition. The position of the anomaly on the  $HT$  phase diagram reported here differs from that of Ref. [27]. We did not find an anomaly in  $M_{dc}(T, H)$  in our samples.

To conclude, the tunnel-diode resonator is proven to have enough sensitivity to measure small changes in the rf penetration depth in the high-field mixed state (i.e. of the Campbell length) which accompany the VL structural transformations. The high-field branch of the rhombic-square lattice transition caused by thermal fluctuation of vortices is mapped up.

We thank J. Yan and G. Lapertot who grew Y1221 crystals in optical furnace. Work at the Ames Laboratory was supported by the Department of Energy-Basic Energy Sciences under Contract No. DE-AC02-07CH11358. R. P. acknowledges support from the NSF grant number DMR-05-53285 and the Alfred P. Sloan Foundation.

---

\* Electronic address: prozorov@ameslab.gov

- [1] J. Schelten, in *Anisotropy Effects in Superconductors* ed. by H. Weber, Plenum, New York, 1977, p.113; B. Obst, *ibid*, p.139.
- [2] D. K. Christen *et al.*, Phys. Rev. B **21**, 102 (1980).
- [3] V. G. Kogan *et al.*, Phys. Rev. Lett. **79**, 741 (1997).
- [4] V. G. Kogan *et al.*, Phys. Rev. B, **55**, R8693 (1997).
- [5] I. Affleck, M. Franz, M.H.S. Amin, Phys. Rev. B **55**, R704 (1997).
- [6] A. Gurevich and V.G. Kogan, Phys. Rev. Lett. **87**, 177009 (2001).
- [7] U. Yaron, *et al.*, Nature (London), **382**, 236 (1996).
- [8] M. R. Eskildsen *et al.*, Phys. Rev. Lett, **78**, 1968 (1997).
- [9] M. Yethiraj *et al.*, Phys. Rev. Lett. **78**, 4849 (1997).
- [10] D. M<sup>c</sup>K. Paul *et al.*, Phys. Rev. Lett. **80**, 1517 (1998).
- [11] Y. De Wilde *et al.*, Phys. Rev. Lett. **78**, 4273 (1997).
- [12] P. L. Gammel *et al.*, Phys. Rev. Lett. **82**, 4082 (1999).
- [13] L.Ya. Vinnikov *et al.*, Phys. Rev. B **64**, 024504 (2001).
- [14] H. Sakata *et al.*, Phys. Rev. Lett. **84**, 15833 (2000).
- [15] M. R. Eskildsen *et al.*, Phys. Rev. Lett, **86**, 5148 (2001).
- [16] M. Laver *et al.*, Phys. Rev. Lett. **96**, 167002 (2006)
- [17] C. E. Sosolik *et al.*, Phys. Rev. B **68**, 140503 (2003).
- [18] M. Yethiraj *et al.*, Phys. Rev. B **72**, 060504 (2005).
- [19] G. Blatter *et al.*, Rev. Mod. Phys. **66**, 1125 (1994).
- [20] A. D. Klironomos and A.T. Dorsey, Phys. Rev. Lett. , **91**, 097002 (2003).
- [21] R. Prozorov *et al.*, Phys. Rev. B **62**, 115 (2000) .
- [22] R. Prozorov *et al.*, Appl. Phys. Lett. **77**, 4202 (2000).
- [23] A. E. Koshelev and V. M. Vinokur, Physica C, **173**, 465 (1991).
- [24] E. H. Brandt, Phys. Rev. Lett. , **67**, 2219 (1991).
- [25] K. O. Cheon *et al.*, Phys. Rev. B, **58**, 6463 (1998).
- [26] X. Y. Miao, S. L. Bud'ko, P. C. Canfield, J. Alloys and

- Comp. **338**, 13 (2002).
- [27] Tuson Park *et al.*, Phys. Rev. B **71**, 054511 (2005).
- [28] P. Miranovic and V.G. Kogan, Phys. Rev. Lett. **87**, 37002 (2001).
- [29] L. D. Landau and E.M. Lifshitz, *Theory of Elasticity*, Pergamon, 1986.